

Supported Nanocomposite Catalysts for High Temperature Reactions: Building a Catalyst from the Nanoparticle Up.

Tom Sanders¹, Mark Kirchhoff, Ullrich Specht, Phae Papas, and Götz Vesper²
Department of Chemical Engineering, University of Pittsburgh, Pittsburgh, PA 15261
Contact: ¹tjs12@pitt.edu or ²gveser@enqr.pitt.edu

Introduction

Nanomaterials have become the focus of intense catalysis research after first reports [1] on nanosized gold particles indicated that nano-scaled materials can show fundamentally different properties from their bulk (macroscopic) equivalent. Furthermore, the extremely large surface-to-volume ratio of nanoparticles makes such materials highly interesting for catalytic applications. However, the thermal stability of particles decreases strongly with decreasing diameter, which currently restricts the application of metallic nanoparticles to low and moderate temperatures ($T < 500^{\circ}\text{C}$).

Previously we have demonstrated the first successful approach to overcome this barrier by anchoring noble metal nanoparticles in a high-temperature stabilized alumina matrix [2, 3]. This synthesis makes use of micelles of a reverse microemulsion as nanoreactors to form a homogenous nanocatalyst [4, 5]. In this way, we were able to synthesize exceptionally active and sinter-resistant platinum-barium hexaaluminate (Pt-BHA) powders which combine the high reactivity of nanosized Pt metal particles with the excellent high-temperature stability of structured aluminas [2, 3, 5-7]. This was the first step in “building” our nanocomposite catalyst. However, concerns with handling of these nanoparticle powders, including health risks and problems with catalyst packing, require an anchoring of the nanocomposite catalyst in a uniform manner onto a support structure as a second “building” step.

We investigated several methods of coating catalyst supports (foams, monoliths, felts) with Pt-BHA gels. Reactive testing, carbon monoxide adsorption, and electron microscopy studies show that quartz glass fiber mats have the most promise as novel support materials to obtain well dispersed Pt-BHA and efficient and stable catalytic activity.

Experimental

Pt-BHA (figure 1) was formed from established procedures [3]. After washing with acetone, the material was freeze-dried, resulting in a gelatinous form which was used in the experiments. Part of the gel was dried to completion and calcined, forming Pt-BHA powder. The powder was sieved and only the fraction with $d > 500$ microns was used in reactive testing. The remaining gelatinous Pt-BHA was used to coat alumina foam monoliths (Vesuvius Hi-Tech Ceramics), cordierite honeycomb monoliths (Corning), and quartz glass mats (Technical Glass Products). Because initial testing of the quartz glass material showed strong catalyst deactivation, all subsequent coatings were done after thermal removal of a chemical binder used in the manufacturing process (482°C , 1 hour 2SLM Air). A 2-3 ml aliquot of the gel was applied to the top of each material and was allowed to settle into the fibrous network and dry in room temperature air. Calcination removed the remaining surfactant and resulted in Pt-BHA coated catalysts. Each calcination was performed in a standard flow through oven (600°C , 3 hours 2SLM air, 3 hours 10% H_2 in N_2 2SLM). Nitrogen and CO adsorption data were obtained on a Micromeritics ASAP 2010.

Reactive testing took place in a quartz-metal hybrid reactor [8]. A quartz glass tube is wrapped in several layers of alumina cloth and inserted into a steel-tube housing. K-type thermocouples are used to monitor reaction temperature on either end of the catalyst bed. The bed is stabilized between two cordierite honeycomb inert zones. Mass flow controllers were used to control the flow of methane and synthetic air for the partial oxidation of methane reaction.

Results and Discussion

SEM images in figure 1 illustrate the shape and size of the powder, and the porous nature of the particle surface ($d_p \sim 1\text{-}10\mu\text{m}$). TEM micrographs (figure 1, right image) reveal the nanoparticles of Pt with diameters around 10 nm which are embedded into a hexaaluminate matrix.

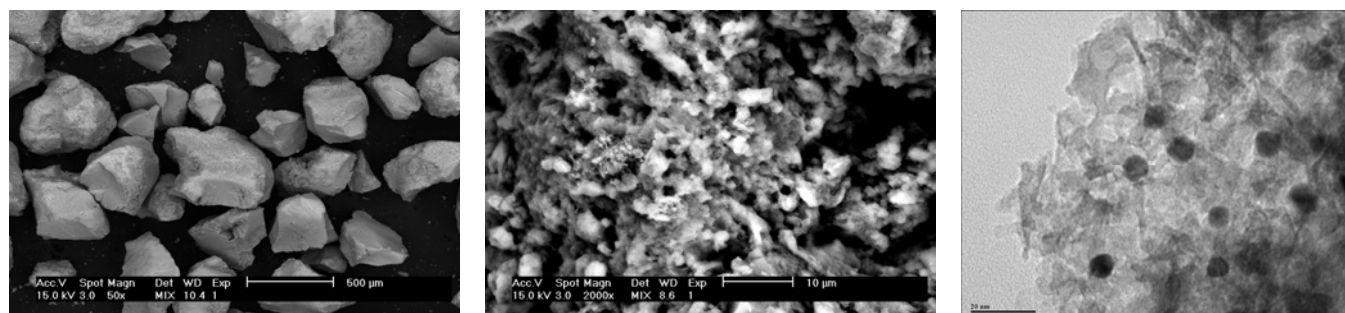


Figure 1: Left: SEM photo showing granules of Pt-BHA calcined at 600°C. Middle: SEM photo showing the porous nature of a granule. Right: TEM micrograph of Pt-BHA showing Pt nanoparticles $d \sim 10\text{nm}$

Figure 2 shows the quartz glass mats before and after coating with the catalytic Pt-BHA. The catalyst is well dispersed amongst the quartz glass fibers as one can see in the center and right images. Vigorous tapping of the catalyst removes a small amount of poorly bound catalytic material, but the majority adheres strongly to the fibers. The other support structures show poor coating tendencies, and are not pictured here.

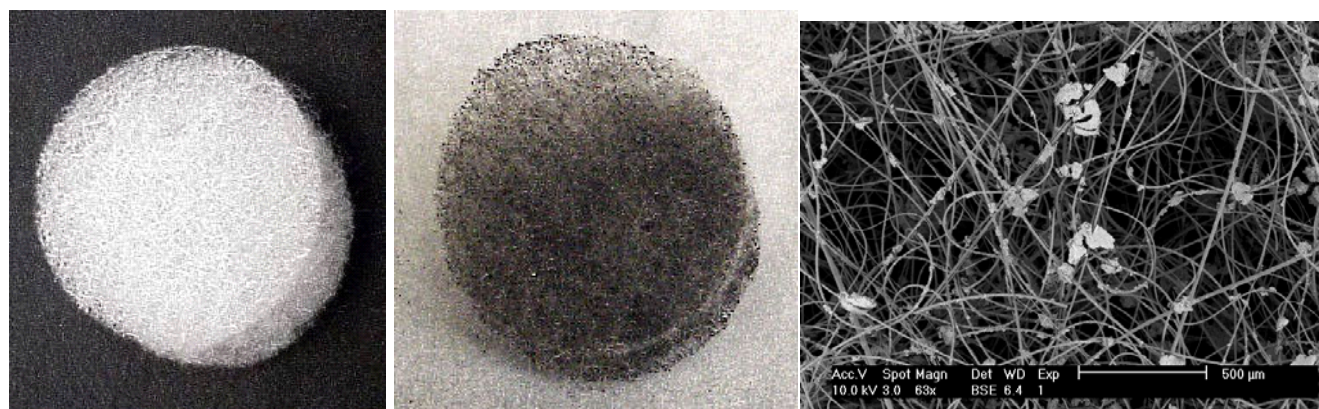


Figure 2: Quartz glass mats. Left: as received. Center: dip coated with Pt-BHA. Right: SEM image of the fibrous network and Pt-BHA material (bright agglomerates)

The hydrogen and carbon monoxide selectivity for the various support structures are shown in figure 3. For hydrogen selectivity, the quartz glass mat is ~8% more selective than the Pt-BHA powder, and as high as ~20% more selective than our standard catalyst (Pt impregnated foam, not shown). The Pt-BHA extruded monolith performs rather poorly, as would be expected from the low dispersion and loading of the Pt-BHA on the surface. The CO selectivity shows an ordering of the supports similar to the trend established in the hydrogen selectivity data.

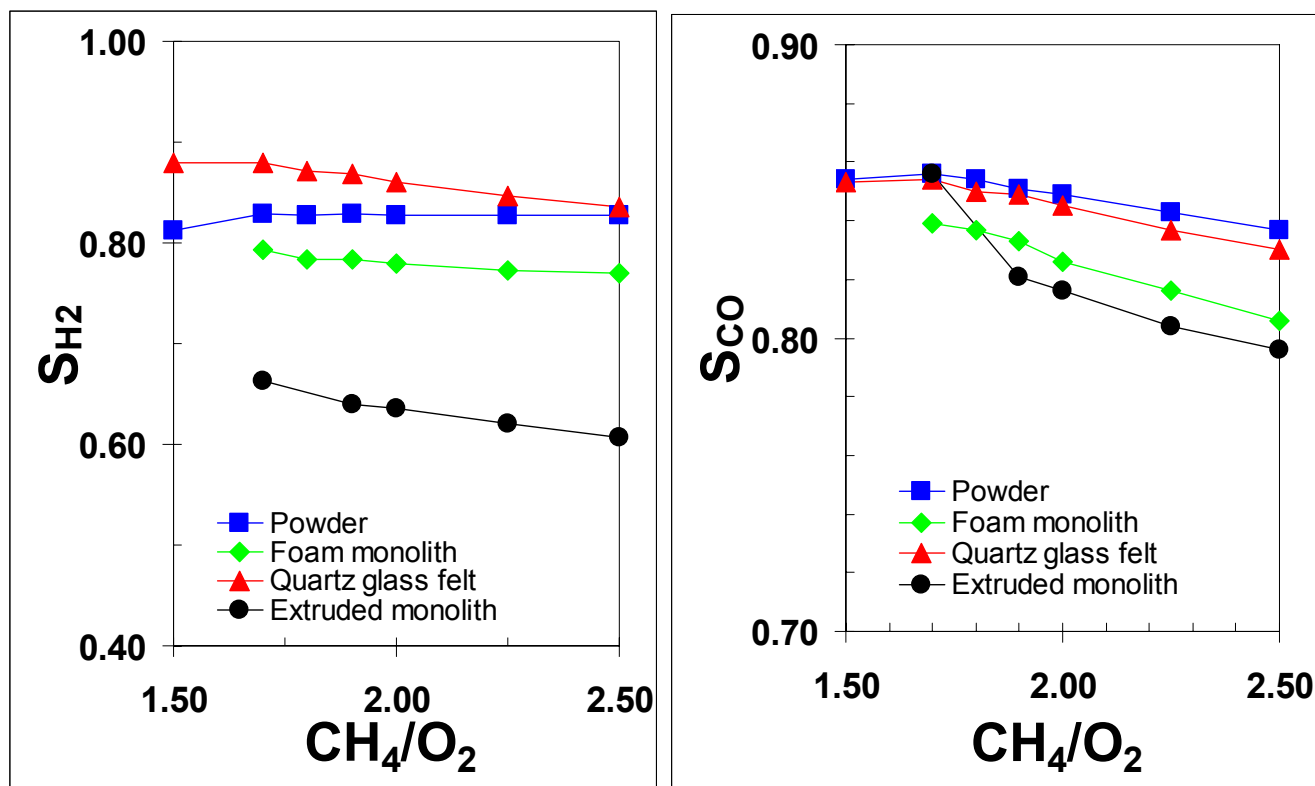


Figure 3: Reactive results for the various support structures. Left: hydrogen selectivity. Right: carbon monoxide selectivity.

Since the quartz glass mat showed the most promising results, it was examined in more detail. The hydrogen selectivity, shown in figure 4, shows a strong increasing trend with increasing Pt-BHA weight loading for the single mats (left graph). At the highest weight loading (0.0841g) the hydrogen selectivity reaches nearly 0.91. By comparison, when 2 mats were used (right graph, figure 4) with a nearly equivalent weight loading (0.0826g), an identical hydrogen selectivity of 0.91 was achieved. Further increases in weight loading (0.099, 0.1415, 0.3229g) showed only modest improvements in hydrogen selectivity (~0.93). When comparing a single mat with 0.0515g Pt-BHA, and 4 mats in series with total 0.0515g Pt-BHA, the results were also remarkably similar (selectivity ~0.87). The reaction is thus limited by the amount of Pt-BHA catalyst and not by the spatial distribution or length of the catalyst bed. At low weight loadings (<0.1g), the reaction is limited by the availability of active sites (i.e. kinetically controlled). At high weight loadings (>0.1g), the reaction becomes mass transfer limited as indicated by the collapse of the curves onto a single curve for loadings above ~0.1g.

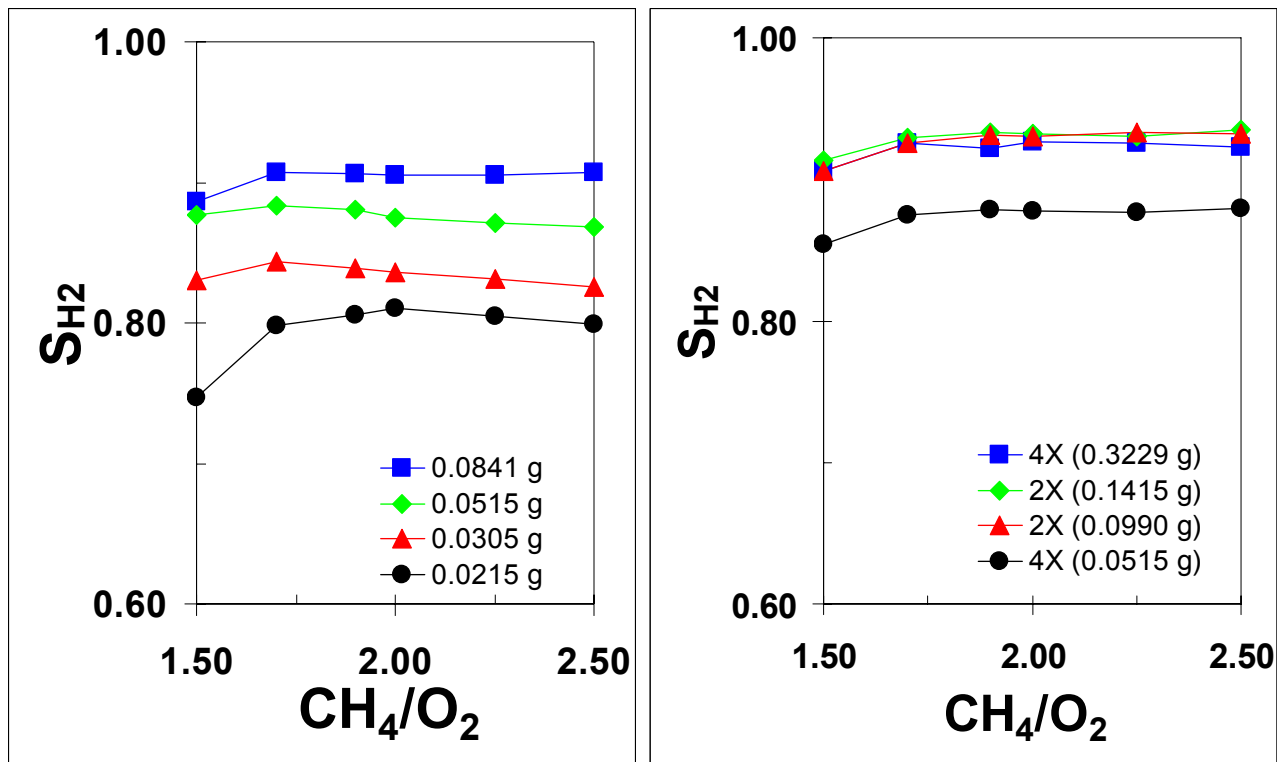


Figure 4: Reactive testing of Pt-BHA coated quartz glass mats. Hydrogen selectivity is plotted as a function of catalyst loading and fuel mixture. Left: single mat Right: multiple mats.

A quantitative comparison of various Pt based catalyst used in the experimental reactive tests is shown in table 1. All materials are disk shaped, leading to characteristic measurements of D=diameter and H=height. One can clearly see the advantage of the nanoparticle character of the catalyst. The Pt-BHA quartz glass mat has approximately 4 times less Pt incorporated, and yet has approximately 5 times the total platinum surface area of the sample drop-coated with platinum salt. In the case of the foam monolith, the Pt-BHA sample has about 11 times less Pt incorporated, but its total platinum surface area only decreases by about a factor of 4. This shows that the Pt-BHA material allows more surface to be available for reaction at a lower total amount of Pt metal, and thus a lower cost.

Table 1: Platinum surface areas measured by CO adsorption for the various supports studied.

Coating	Structure	Size (mm)	wt Pt (mg)	a_{Pt} (m^2/g)		A_{Pt} (m^2)
				(g Pt)	(g cat)	
10% H_2Cl_6Pt	Foam Monolith	D=18, H=10	62.8	4.68	0.14	0.294
	Quartz Glass	D=20, H=2	20.1	0.96	0.42	0.0192
Pt-BHA	Foam Monolith	D=18, H=10	2.7	29.62	0.03	0.080
	Powder Bed	D=18, H=3	38.0	57.40	4.31	2.18
	Quartz Glass	D=20, H=2	4.9	19.81	1.15	0.096

Conclusion

Quartz glass mat-supported Pt-BHA catalysts showed strongly improved synthesis gas yields in partial oxidation of methane with *orders of magnitude* in reduction in the Pt content in comparison to traditional Pt/Al₂O₃ catalysts. The Pt-BHA powder is high-temperature stable over long periods of reaction (100 hours in previous testing), and initial tests show promise for the supported Pt-BHA. Overall, we therefore see a great potential for these catalysts for energy applications, in particular the production of synthesis gas and/or hydrogen from methane via steam reforming, autothermal reforming or partial oxidation.

Literature

1. Haruta, M., *Size- and support-dependency in the catalysis of gold*. Catalysis Today, 1997. **36**(1): p. 153-166.
2. Schicks, J., et al., *Nanoengineered catalysts for high-temperature methane partial oxidation*. Catalysis Today, 2003. **81**(2): p. 287-296.
3. Kirchhoff, M., U. Specht, and G. Vesper, *Engineering high-temperature stable nanocomposite materials*. Nanotechnology, 2005. **16**(7): p. S401-S408.
4. Pileni, M.P., *Reverse Micelles as Microreactors*. Journal of Physical Chemistry, 1993. **97**(27): p. 6961-6973.
5. Zarur, A.J. and J.Y. Ying, *Reverse microemulsion synthesis of nanostructured complex oxides for catalytic combustion*. Nature, 2000. **403**(6765): p. 65-67.
6. Zarur, A.J., et al., *Phase Behavior, Structure, and Applications of Reverse Microemulsions Stabilized by Nonionic Surfactants*. Langmuir, 2000. **16**(24): p. 9168-9176.
7. Zarur, A.J., H.H. Hwu, and J.Y. Ying, *Reverse Microemulsion-Mediated Synthesis and Structural Evolution of Barium Hexaaluminate Nanoparticles*. Langmuir, 2000. **16**(7): p. 3042-3049.
8. Neumann, D., V. Geper, and G. Vesper, *Some Considerations on the Design and Operation of High-Temperature Catalytic Reverse-Flow Reactors*. Ind. Eng. Chem. Res., 2004. **43**: p. 4657-4667.